Thiamine Hydrochloride as a Potential Inhibitor for Aluminium Corrosion in 1.0 M HCl: Mass Loss and DFT Studies

Mamadou Yeo, Paulin Marius Niamien*, Ehui Bernadette Avo Bilé, Albert Trokourey

Laboratoire de chimie physique, Université Félix Houphouët Boigny

ABSTRACT

Thiamine hydrochloride (vitamin B1) has been tested as a potential inhibitor for aluminium corrosion in 1.0 M hydrochloric acid solution, using mass loss technique and DFT studies. These studies were performed in the concentration range of 0.13 mM to 0.53 mM and the temperature range of 303 K to 323 K. The experimental results show that the inhibition efficiency is concentration and temperature dependent. Experimental data were used to fit adsorption isotherms including Langmuir, El-Awady, Freundlich and Temkin. Though the Langmuir model was the appropriate isotherm, it could not be applied rigorously. Furthermore, the Adejo-Ekwenchi isotherm was used to characterize the type of adsorption. The thermodynamic adsorption and activation functions were determined and analysed. They indicate a spontaneous adsorption process and both physisorption and chemisorption processes. Density functional theory (DFT) calculations were performed and discussed. They reveal good correlations between experimental and theoretical results.

Keywords: Aluminium, Hydrochloric acid solution, Thiamine hydrochloride, Corrosion inhibition, Mass loss technique, Density functional theory

INTRODUCTION

Aluminium [1,2] is widely used in many applications in a broad field of industry (automobiles, aviation, containers, electronic devices, etc.). It is generally [2] covered by a thin oxide film, which protects it from corrosion in various environments. However, when being in contact with acids such as hydrochloric acid, sulphuric acid, etc., it undergoes corrosion.

The most practical method [3-5] used to combat aluminium acid corrosion is the use of organic corrosion inhibitors (e.g. addition of heterocyclic organic compounds in the metal's environment). Up to now, various organic compounds containing heteroatoms such as O, N and S have been reported to be good inhibitors for aluminium corrosion in HCl media. Indeed, it is generally accepted [6-8] that organic compounds exert their inhibitory action via adsorption on metal surface through the heteroatoms and their double bonds in the aromatic rings.

The adsorption of the organic compounds onto the metal surface is influenced by their chemical structures. The use of quantum chemical calculations [9] leads to structural and reactivity parameters of molecules. Many studies in the literature [10-12] have reported on the use of DFT calculations in aluminium acid corrosion inhibition. It is revealed that the inhibitory action of the organic compounds is correlated with the theoretical parameters such as the highest occupied molecular orbital energy (E_{HOMO}), the lowest unoccupied molecular orbital energy (E_{LUMO}), the energy gap ΔE, the dipole moment μ, the Mulliken atomic charges, etc. Actually, the choice of effective corrosion inhibitors [13,14] is generally based on the correlation between experimental data (inhibition efficiency from mass loss or/ and electrochemical studies) and the quantum chemical properties (electron donating or/and accepting ability) of the studied molecules.

In the present work, the inhibitory effect of Thiamine hydrochloride (thiamine chloride in hydrochloric environment)

on aluminium corrosion in 1.0 M HCl solution is investigated by mass loss technique and quantum chemical calculations based on density functional theory (DFT), which is used to get insight into the corrosion inhibition mechanism.

MATERIALS AND METHODS

Materials

Aluminium specimens

The aluminium specimens were in the form of rod measuring 10 mm in length and 2 mm in diameter; they were cut in commercial aluminium of purity 99.5%.

Chemicals

All chemicals were of analytical grade and were used without further purification:

- HCl from Merck with purity: 37%

- Thiamine hydrochloride *($C_{12}H_{17}ClN_4OS,HCl$)* of purity 99% was acquired from Sigma Aldrich chemicals and solutions of concentrations range from 0.13 mM to 0.53 mM were prepared.

- Acetone from Sigma Aldrich with purity: 99.5%

Methods

Mass loss experiments

The mass loss experiments were performed using an electrical balance (accuracy: 0.01 mg). The samples were polished, cleaned with acetone, washed with bidistilled water, dried, weighed and then immerged in the test solutions without or with different concentrations of thiamine hydrochloride, for different temperatures. After one hour immersion in 50 mL of the test solutions, the specimens were retrieved from the solution, washed with a bristle brush under running water in order to remove the corrosion product, dried in a desiccator and weighed accurately.

For each case, a triplicate experiment was conducted. The average mass loss was then used to calculate the corrosion rate, which was expressed by:

$$W = \frac{\Delta m}{St} \tag{1}$$

Where Δm is the mass loss, S is the total surface of the sample and t is the immersion time. The inhibition efficiency was calculated using the following equation:

$$IE\left(\%\right) = \frac{W_0 - W}{W_0} \times 100 \tag{2}$$

In this equation, W_0 is the corrosion rate without the investigated compound and W is the corrosion rate in presence of thiamine hydrochloride.

Quantum chemical calculations

The quantum chemical calculations were performed to establish some correlations between the molecular structure and the inhibition efficiency of the investigated molecule. The calculations were performed using the Gaussian 03W package [15]. The gradient corrected functional theory (DFT) with the three parameter hybrid functional of Becke 3 (B3) for the exchange part and the Lee-Yang-Parr (LYP) functional [16]; with the basis set 6-31G (d) was used to determine the structural and reactivity parameters of the molecule. The calculations were carried out in the gas phase to show the relationship between the molecular descriptors and the inhibition efficiency of the studied compound. The optimized (minimum energy) geometrical configuration of Thiamine chloride is given in Figure 1.
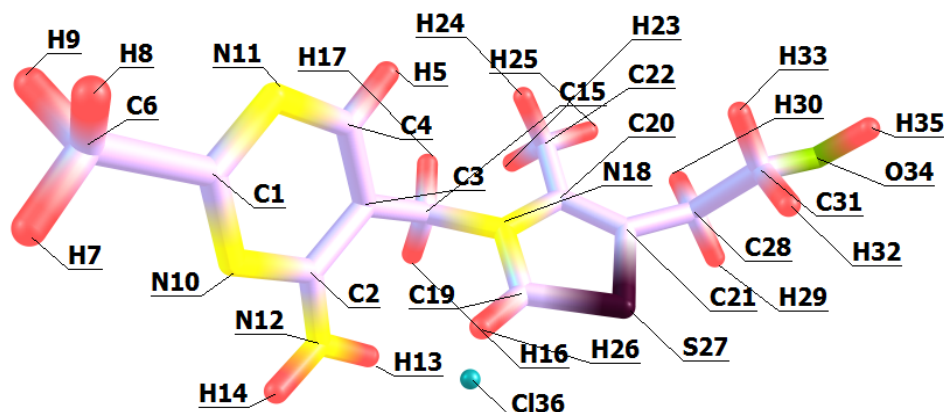
Figure 1: optimized structure of thiamine chloride by DFT B3LYP/6-31G (d)

The molecular descriptors such as E_{HOMO} (the energy of the highest occupied molecular orbital), E_{LUMO} (the energy of the lowest unoccupied molecular orbital), the HOMO-LUMO energy gap, the dipole moment μ and the total energy *TE* of the molecule were computed. The reactivity parameters were then calculated using the conceptual framework of DFT [17,18]. So, the chemical potential μ_p is defined as:

$$\mu_P = \left(\frac{\partial E}{\partial N}\right)_{v(r)} = -\chi \tag{3}$$

Where *x* is the global electronegativity, while the global hardness is given by the equation below:

$$\eta = \left(\frac{\partial^2 E}{\partial N^2}\right)_{v(r)} \tag{4}$$

Using the finite difference approximation and the Koopmans theorem, the global electronegativity and the global hardness can be written as:

$$\chi = \frac{(I+A)}{2} \approx -\frac{(E_{HOMO} + E_{LUMO})}{2} \tag{5}$$

$$\eta = \frac{(I-A)}{2} \approx -\frac{(E_{HOMO} - E_{LUMO})}{2} \tag{6}$$

The global softness which is the reciprocal of the global hardness is given by the following equation:

$$S = \frac{1}{\eta} = \frac{2}{(I-A)} \tag{7}$$

The electrophilicity index ω [19] is defined as:

$$\omega = \frac{\mu_P^2}{2\eta} = \frac{(I+A)^2}{4(I-A)} \tag{8}$$

In relations (5) to (8), *I* and *A* are respectively the ionization energy and the chemical affinity.

The fraction of electrons transferred (ΔN) is given by the following equation [20]:

$$\Delta N = \frac{\phi_{Al} - \chi_{inh}}{2(\eta_{Al} + \eta_{inh})} \tag{9}$$

The values of experimental work function ϕ_{Al} =4.28 *eV* [21] and hardness η_{Al} = 0 [22] (since for bulk metallic atoms *I* = *A*) were considered to calculate ΔN.

The Fukui function [17] is defined as the derivative of the electronic density ρ(r) with respect to the number *N* of electrons:

$$f(r) = (\frac{\partial \rho(r)}{\partial N})_{v(r)} \tag{10}$$

The Fukui function *f* (*r*) reflects the ability of a molecular site to accept or donate electrons. High values of *f* (*r*) [17] are associated to a high reactivity at point *r*. Equation (10) associated with a finite difference approximation leads to two definitions of Fukui functions depending on total electronic densities:

$$f^+(r) = \rho_{N+1}(r) - \rho_N(r) \tag{11}$$

$$f^-(r) = \rho_N(r) - \rho_{N-1}(r) \tag{12}$$

Where $\rho_{N+1}(r)$, $\rho_N(r)$ and $\rho_{N-1}(r)$ are the electron densities at point *r* for the system with $N + 1$, N and $N - 1$ electrons, respectively.

The function $f^+(r)$ measures the reactivity at the site *r* towards nucleophilic attacks, while $f^-(r)$ measures the reactivity at the site *r* towards electrophilic attacks.

Actually, a new descriptor has been introduced [23,24] which allows the determination of individual sites within the molecule with particular behaviours. This descriptor is defined as:

$$\Delta f(r) = \left(\frac{\partial f(r)}{\partial N} \right)_{v(r)} \tag{13}$$

The condensed form [23] of the dual descriptor is given by the equation below:

$$\Delta f(r) = f_k^+ - f_k^- \tag{14}$$

When, $\Delta f_k(r) > 0$, the process is driven by a nucleophilic attack and atom *k* acts as an electrophile; conversely, when, $\Delta f_k(r) < 0$, the process is driven by an electrophilic attack on atom *k* acts as a nucleophile. $\Delta f(r)$ is defined within the range {-1;1}, what makes interpretation easy [25].

RESULTS AND DISCUSSION

Mass loss studies

Figures 2 and 3 present the inhibition efficiency of Thiamine hydrochloride (Thiamine chloride in hydrochloric environment), respectively versus concentration and temperature.
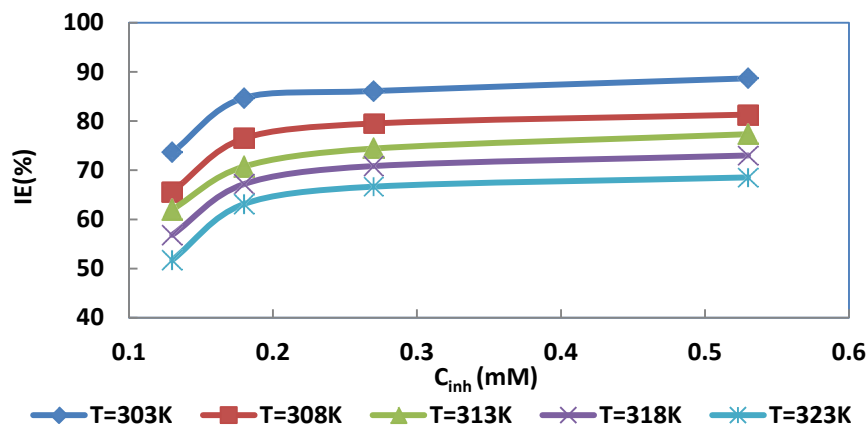

Figure 2: Inhibition efficiency of thiamine hydrochloride versus concentration for different temperatures
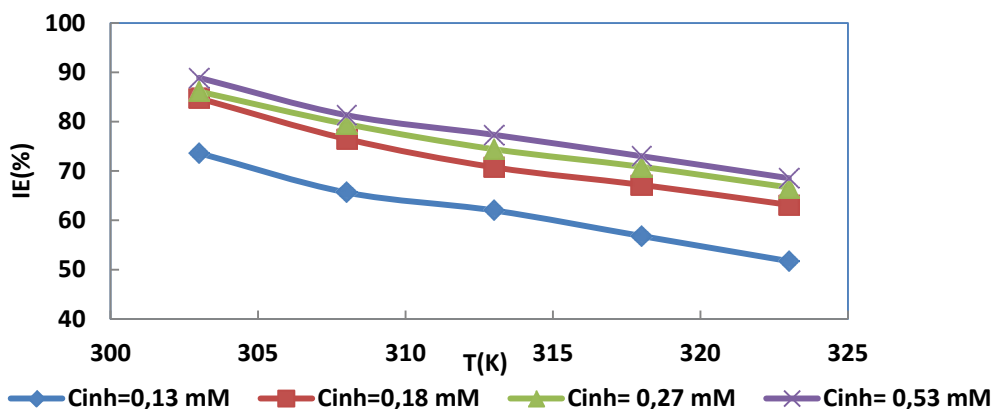
Figure 3: Inhibition efficiency of thiamine hydrochloride versus temperature for different concentrations

From Figure 2, it is clear that the inhibition efficiency of Thiamine hydrochloride increases with the rise in its concentration. This result suggests that the studied compound inhibit the corrosion of aluminium in HCl for all the range of the used concentrations to different degree. The increase in inhibition efficiency with increasing concentration [26] indicates that the corrosion inhibition process is attributed to the adsorption of the inhibitor onto the metal surface: a barrier could be formed which separates the metal surface from its aggressive environment.

Analysing Figure 3, one can see that the inhibition efficiency decreases with increasing temperature, probably due to desorption of the inhibitor molecules when the temperature increases.

Adsorption isotherms and thermodynamic consideration

Adsorption isotherms [27] are very important in understanding the interaction between a metal and an inhibitor. The isotherms are in general form:

$$K_{ads}C_{inh} = g(\theta, x)\exp(-f\theta) \tag{15}$$

Where, $g(\theta,x)$ is the configurational factor subject to the physical model and assumptions involved in the derivation of the isotherms, C_{inh} is the inhibitor concentration, θ is the surface coverage, K_{ads} is the equilibrium constant of the adsorption process and f is a parameter that expresses the interaction of the molecules in the adsorbed layer.

The experimental data were used to fit several isotherms including Langmuir, El-Awady, Freundlich and Temkin. It was found that the data suit well with Langmuir adsorption isotherm. Figure 4 gives the plots associated with the Langmuir isotherm. Though this isotherm presents high correlation coefficient values, the deviation of the slopes from unity shows that this model cannot be applied rigorously.
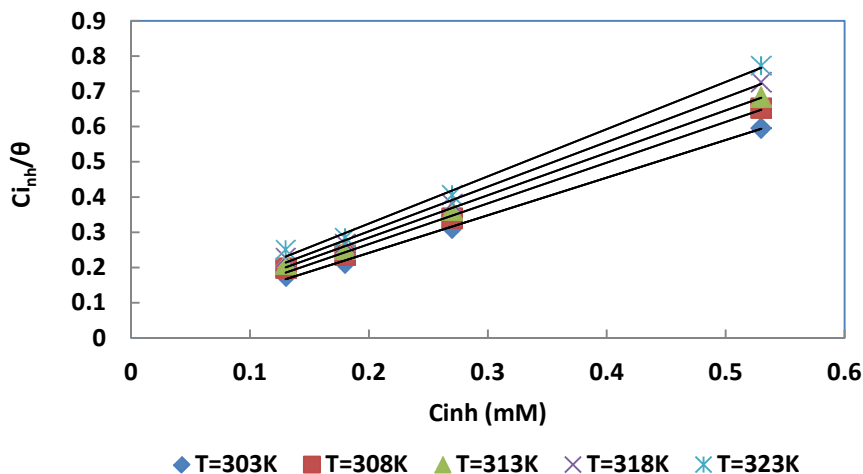

Figure 4: Langmuir adsorption plots for the adsorption of thiamine hydrochloride onto aluminium in 1.0 M HCl

To solve the problem, one can use the modified form of the Langmuir isotherm also called Villamil adsorption isotherm [28]. This isotherm is described by the following equation:

$$\frac{C_{inh}}{\theta} = \frac{n}{K_{ads}} + nC_{inh}$$

(16)

Table 1 presents the adsorption parameters of Langmuir isotherm.

Table 1: Adsorption parameters of modified Langmuir isotherm

Isotherm	T (K)	R^2	Slope	Intercept	$K_{ads}\left(M^{-1}\right)$	$\Delta G^0_{ads}\left(kJmol^{-1}\right)$
	303	0.998	1.0669	0.0029	35600	-36.5
	308	0.998	1.1557	0.0355	28900	-36.6
Villamil	313	0.999	1.2054	0.0436	30100	-37.3
	318	0.997	1.2684	0.0490	25300	-37.4
	323	0.995	1.3394	0.0571	22320	-37.6

The change in adsorption enthalpy was calculated using the equation:

$$\Delta G^0_{ads} = -RTln\left(55.5 \times K_{ads}\right)$$

(17)

Where R is the perfect gas constant, T is the absolute temperature and 55.5 is the concentration (in mol L⁻¹) of water in the solution.

To get insight into the knowledge of the type of adsorption, we use the Adejo-Ekwenchi isotherm [29]. This isotherm is characterized by the equation below:

$$\log\left(\frac{1}{1-\theta}\right) = logK_{AE} + blogC_{inh}$$

(18)

Where C_{inh} is the concentration of the adsorbate, K_{AE} and b are the isotherm parameters. Figure 5 gives the plots of log $(1/1-\theta)$ versus log C_{inh}.
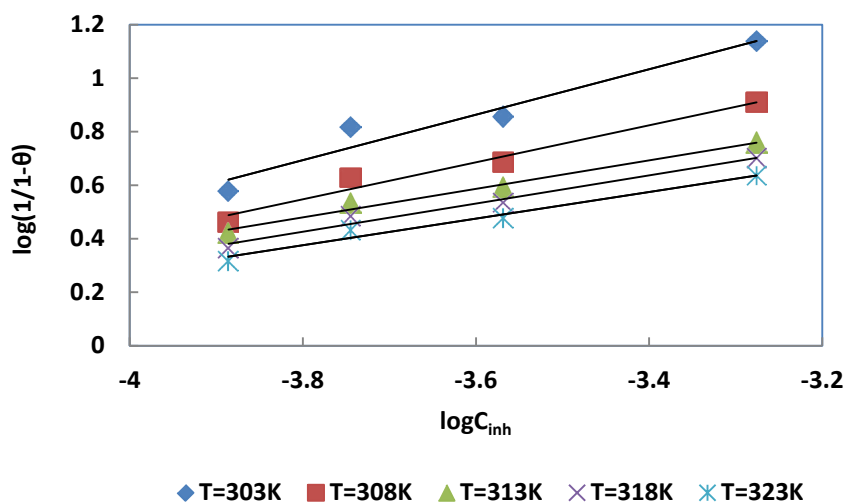

Figure 5: Plots of Adejo-Ekwenchi adsorption isotherm for thiamine hydrochloride onto aluminium in 1.0M HCl

The parameters of Adejo-Ekwenchi isotherm are listed in Table 2.

Table 2: Parameters of the Adejo-Ekwenchi isotherm plots

T(K)	R^2	b	Intercept	$\Delta G^0_{ads}\left(kJmol^{-1}\right)$
303	0.946	0.8495	3.9222	-32.85
308	0.972	0.6916	3.1758	-29.00
313	0.984	0.5331	2.5054	-25.45
318	0.979	0.5262	2.4260	-25.37
323	0.974	0.4972	2.2647	-24.78

From Table 2, one can see that the values of ΔG^0_{ads} are in the same range (-20 kJ mol⁻¹ to -40 kJ mol⁻¹) as that obtained with the Langmuir adsorption isotherm.

To obtain the values of change in enthalpy ΔH^0_{ads} and change in entropy, the basic thermodynamic equation below was used:

$$\Delta G^0_{ads} = \Delta H^0_{ads} - T\Delta S^0_{ads} \tag{19}$$

Plotting ΔG^0_{ads} versus temperature (in the case of the modified Langmuir adsorption isotherm (Figure 6), we obtain a straight line with a slope of (-ΔS^0_{ads}) and an intercept of (ΔH^0_{ads}).
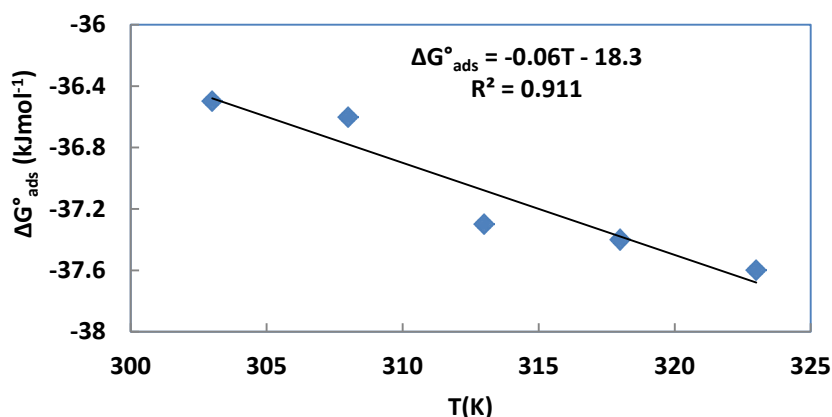

Figure 6: ΔG^0_{ads} versus temperature in the case of modified Langmuir isotherm

The values of change in adsorption free energy ΔG^0_{ads} are negative, showing the spontaneous character of the adsorption. From the equation of the straight line, we deduce the values of change in adsorption enthalpy $\Delta H^0_{ads} = $ -18.3 *kJ mol⁻¹* and that of change in adsorption entropy $\Delta S^0_{ads} = 60$ *J mol⁻¹ K⁻¹*. The negative sign of change in adsorption enthalpy indicates an exothermic adsorption process while the positive sign of ΔS^0_{ads} shows that disorder increases probably due to desorption of water molecules.

The obtained values of ΔG^0_{ads} are included in the range of -40 *kJ mol⁻¹* to -20 *kJ mol⁻¹* indicating the existence of both physisorption and chemisorption [30]. It can be seen from Table 2 that the parameter *b* in the Adejo-Ekwenchi isotherm decreases when going from T = 303 *K* to, *T* = 308 *K* indicating [31] a physisorption process. For *T* = 313 *K* to *T* = 323 K, the values of the parameter *b* are fairly constant, indicating [31] a chemisorption process.

Effect of temperature

To calculate the kinetic and thermodynamic parameters of the dissolution process of the aluminium, Arrhenius equation (20) and the transition state equation (21) were used:

$$logW = logA - \frac{E_a}{2.303RT} \tag{20}$$

$$log\left(\frac{W}{T}\right) = log\left(\frac{R}{\aleph h}\right) + \frac{\Delta S^*_a}{2.303R} - \frac{\Delta H^*_a}{2.303RT} \tag{21}$$

Where E_a is the apparent activation energy, *R* is the molar gas constant, *A* is the frequency factor, *h* is the Planck's constant, $\aleph$ is the Avogadro number, ΔS^*_a is the change in activation entropy and ΔH^*_a is the change in activation enthalpy.

Figure 7 gives the plots of *logW* versus 1/T; the values of the apparent activation energy are deduced from the slopes of the straight lines and the values of the frequency factor *A* are calculated using the intercepts. All the calculated parameters are listed in Table 3.

The higher values of activation energy E_a in the presence of thiamine hydrochloride when compared with that in its absence and the decrease of inhibition efficiency with rise in temperature [32,33] indicate the predominance of the physisorption process.

Table 3: Dissolution parameters of aluminium in 1.0 M HCl without and with various concentrations of thiamine hydrochloride

System/Concentration	$E_a \left(\text{kJ mol}^{-1} \right)$	$\Delta S_a^* \left(\text{J mol}^{-1}\, \text{K}^{-1} \right)$	$\Delta S_a^* \left(\text{J mol}^{-1}\, \text{K}^{-1} \right)$
Blank	81.0	78.6	-24.2
0.13 mM	103.5	101.1	39.5
0.18 mM	114.0	111.5	69.9
0.27 mM	114.2	111.8	70.9
0.53 mM	119.5	117.0	85.6
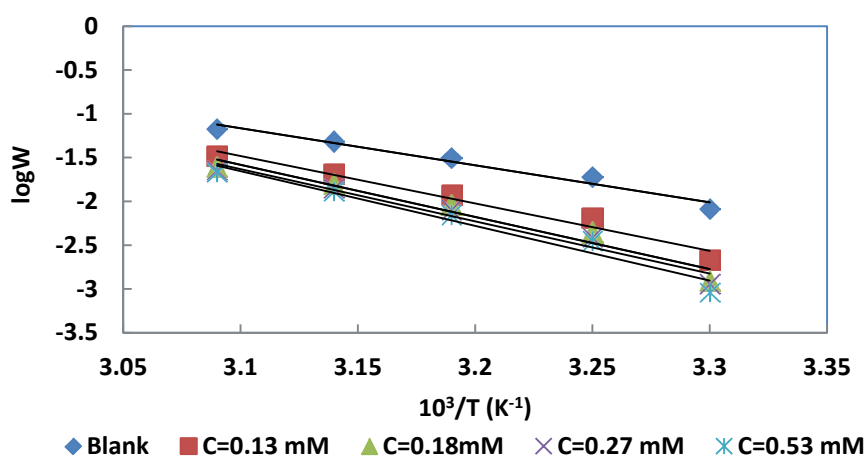
Figure 7: Arrhenius plots for the dissolution of aluminium in 1.0 M HCl without or with various concentrations of thiamine hydrochloride

The values of change in activation enthalpy ΔH_a^* and that of change in entropy were obtained by plotting $\log(W/T)$ versus $1/T$. Figure 8 gives the plots without and with different concentrations of thiamine hydrochloride. The plots of $\log(W/T)$ versus $1/T$ are straight lines with slopes of $(-\Delta H_a^*/2.303\text{R})$ and intercept of $[\log(\text{R}/\aleph h) + \Delta S_a^*/20303R]$ from which we deduced respectively ΔH_a^* and ΔS_a^* (Table 3). From Table 3, one can observe that the values of change in activation enthalpy for the dissolution of aluminium in 1.0 M HCl in presence of thiamine hydrochloride is higher than that in the absence of the inhibitor. The values increase with increasing concentration in the inhibitor: the dissolution of the aluminium is more and more difficult when the concentration in inhibitor increases.
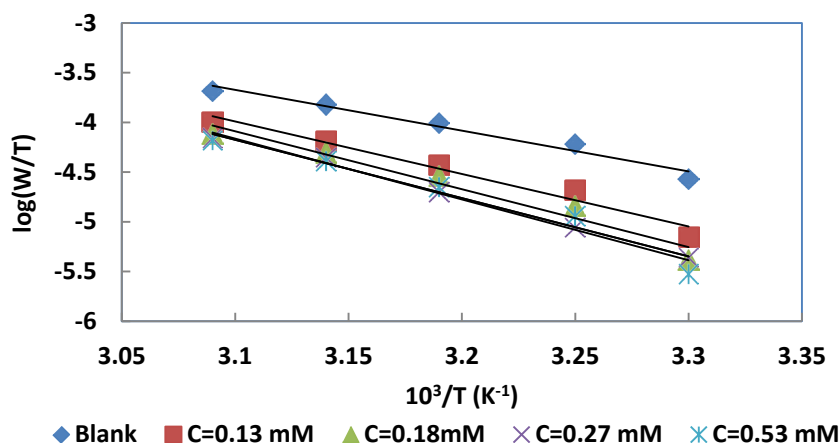
Figure 8: Transition state plots for aluminium dissolution in the absence and presence of various concentrations of thiamine hydrochloride

The positive sign of ΔH_a^* reflects [34] the endothermic nature of the aluminium dissolution, which is slow in the presence of the inhibitor. An inspection of Table 3 shows that the activation energy E_a and the change in activation

enthalpy ΔH^*_a values vary in the same way. We can verify the known thermodynamic relation between the two parameters:

$$\Delta H^*_a = E_a - RT \tag{22}$$

The change in activation entropy is positive in the absence and presence of the inhibitor, indicating that the rate-determining step for the activated complex is dissociation rather than an association. The dissolution process is accompanied by an increase in entropy, probably due to desorption of the adsorbed species. Similar observation [35] has been reported in the literature.

Quantum chemical calculations

The calculated quantum chemical parameters are collected in Table 4.

Table 4: Quantum chemical parameters of thiamine chloride

Descriptor	Value	Descriptor	Value
$E_{HOMO}\,(eV)$	-5.838	$E_{LUMO}\,(eV)$	2.078
$E_{LUMO}\,(eV)$	-1.681	$S(eV)^{-1}$	0.481
$\Delta E\,(eV)$	4.157	$\mu\,(Debye)$	7.551
ΔN	5.838	ΔN	0.125
$A\,(eV)$	1.681	$\omega\,(eV)$	3.399
$\chi\,(eV)$	3.759	$TE\,(a.\,u.)$	-1620.1

The frontier molecular orbital (FMO) theory states that the reactive ability of an inhibitor is closely related to the HOMO and LUMO energies. Higher value of E_{HOMO} for a molecule [36] indicates its electron-donating ability to an appropriate acceptor with low empty energy orbital. In our case the HOMO energy (E_{HOMO}=-5.838 eV) which can be considered as a high value when compared with values in the literature [37] could explain the high inhibition efficiency of the studied molecule.

The LUMO energy orbital is associated to electron accepting ability of a molecule. Lower value of E_{LUMO} for a molecule [38] signifies good electron accepting ability. The obtained value (E_{LUMO}=-1.681 eV) is low when compared with that of some molecules in the literature [39]; so, the studied molecule could receive electrons from the aluminium metal.

The HOMO-LUMO gap, i.e., the difference in energy between the HOMO and LUMO ($\Delta E = E_{LUMO}-E_{HOMO}$) is an important stability index. A large HOMO-LUMO gap [40] implies a high stability for the molecule in chemical reactions. In our case, the low value of energy gap ($\Delta E = 4.157\ eV$) could explain the high inhibition efficiency value (IE (%)=88.69 for C_{inh}=0.53 mM at T = 303 K). HOMO and LUMO of the inhibitor are given in Figure 9.
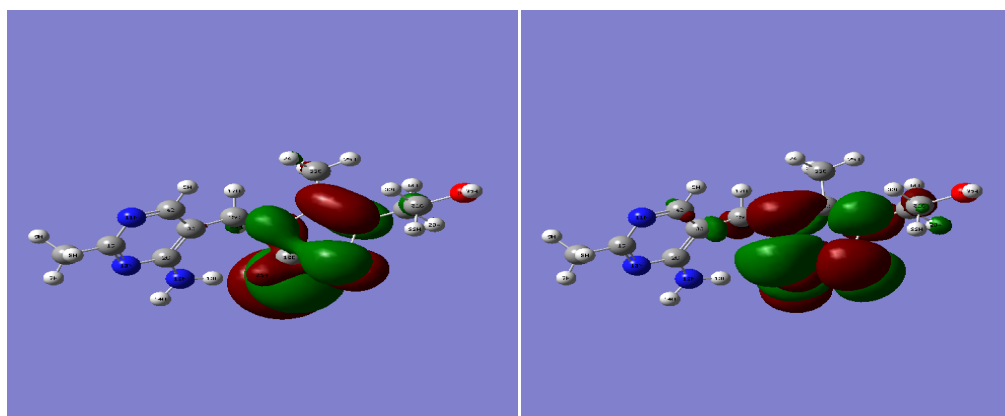

Figure 9: HOMO (left) and LUMO (right) of thiamine chloride by B3LYP/6-31G (d)

From Figure 9, it can be seen that the HOMO and LUMO of the studied molecule are in the region containing the chloric atom and the cycle in which we have the sulphur atom. So, this region is probably the active area where transfers of electrons could be done (from the molecule to aluminum or vice-versa).

Ionization energy I and electron affinity A are two important parameters associated with the HOMO and LUMO energies. Low ionisation energy and high electron affinity, generally [41] lead to good inhibition properties. In our case, the low ionisation energy (I = 5.838 eV) could explain the high inhibition efficiency.

The dipole moment (μ) is another important parameter which measures the assymetry in molecular charge distribution. It provides information about the polarity of a molecule. However, there is no consensus concerning the correlation between the dipole moment and inhibitive effectiveness [42]. According to some authors, low values of dipole moment favour inhibitor molecules accumulation on the surface thus increasing inhibition efficiency [43,44]. On the other hand some researchers states that a high value of dipole moment lead to a good inhibition efficiency of an organic molecule [45].

Electronegativity (χ), hardness (η) and softness (S) [46] are very useful quantities in chemical reactivity theory. Electronegativity indicates the capacity of a system to attract electrons, whereas hardness and softness express the degree of reactivity of the system. In our study, the electronegativity of the studied molecule(χ_{inh} = 3.759 eV) is lower than the metal's work function (ϕ_{Al} = 4.28 eV), showing that aluminium has the better attraction capacity. This situation leads to a positive value of electron transferred (ΔN = 0.125) indicating a possible motion of electrons from the inhibitor to the metal.

The electrophilicity index (ω) [47] measures the propensity of chemical species to accept electrons; a high value of electrophilicity index describes a good electrophile while a small value of electrophilicity describes a good nucleophile. In our case the high value (ω = 3.399 eV) expresses the electrophile character of the studied molecule showing the possible transfer of electrons from the metal to the inhibitor.

The Mulliken charge distribution of the studied molecule with calculated Fukui functions are presented in Table 5, form there it is clear that C (6), N (10), N (11), N (12), N (18), C (19), C (27), C (28) and O (34) have high charge densities. Therefore, they are active centres (adsorption centres), which could have strongest ability to bond the metal surface. In our case, the neutral form of the inhibitor could use these active centres to adsorb on the aluminium surface [48].

The local reactivity of the studied molecule is analysed via the condensed Fukui functions and the dual descriptor (Table 5). These functions help to distinguish each part of the molecule according to its behaviour due to the different functional groups. Thus the site for nucleophilic attack will be the site where f_k^+value is maximum and $\Delta f_k(r)$ is positive whereas the site for electrophilic attack will be the site where f_k^- is maximum and $\Delta f_k(r)$is negative.

Table 5: Calculated Mulliken atomic charges, Fukui functions and dual descriptor by DFT B3YLP6-31/ G (d)

Atom	q_{N+1}	q_N	q_{N-1}	f_k^+	f_k^-	$\Delta f_k(r)$
1 C	0.388442	0.397112	0.406223	-0.008670	-0.009111	0.000441
2 C	0.232468	0.294956	0.313167	-0.062488	-0.018211	-0.044277
3 C	0.078027	0.050240	0.037632	0.027787	0.012608	0.015179
4 C	-0.006136	0.046681	0.033312	-0.052817	0.013369	-0.066186
5 H	0.163288	0.205300	0.186634	-0.042012	0.018666	-0.060678
6 C	-0.491046	-0.492772	-0.494366	0.001726	0.001594	0.000132
7 H	0.146528	0.182901	0.207457	-0.036373	-0.024556	-0.011817
8 H	0.152117	0.184940	0.201878	-0.032823	-0.016938	-0.015885
9 H	0.151062	0.180389	0.196990	-0.029327	-0.016601	-0.012726
10 N	-0.516521	-0.454785	-0.423397	-0.061736	-0.031388	-0.030348
11 N	-0.505536	-0.431301	-0.410874	-0.074235	-0.020427	-0.053808
12 N	-0.773559	-0.746893	-0.725373	-0.026666	-0.021520	-0.005146
13 H	0.298879	0.323969	0.331458	-0.025090	-0.007489	-0.017601
14 H	0.300169	0.333131	0.347747	-0.032962	-0.014616	-0.018346
15 C	-0.185571	-0.189986	-0.210024	0.004415	0.020038	-0.015623
16 H	0.115011	0.162410	0.197169	-0.047399	-0.034759	-0.012640

17 H	0.148293	0.189361	0.223641	-0.041068	-0.034280	-0.006788
18 N	**-0.386513**	**-0.395075**	**-0.378924**	**0.008562**	**-0.016151**	**0.024713**
19 C	**-0.265980**	**-0.209397**	**-0.244739**	**-0.056583**	**0.035342**	**-0.091925**
20 C	0.260856	0.260055	0.314860	0.000801	-0.054805	0.055606
21 C	-0.216508	-0.203055	-0.205165	-0.013453	0.002110	-0.015563
22 C	-0.511443	-0.509308	-0.512267	-0.002135	0.002959	-0.005094
23 H	0.147711	0.178359	0.226047	-0.030648	-0.047688	0.017040
24 H	0.146809	0.159152	0.199146	-0.012343	-0.039994	0.027651
25 H	0.154618	0.185476	0.221548	-0.030858	-0.036072	0.005214
26 H	0.214091	0.236307	0.308769	-0.022216	-0.072462	0.050246
27 S	0.167677	0.284053	0.484865	-0.116376	-0.200812	0.084436
28 C	-0.299981	-0.307698	-0.317959	0.007717	0.010261	-0.002544
29 H	0.146739	0.180535	0.227527	-0.033796	-0.046992	0.013196
30 H	0.134837	0.163056	0.202905	-0.028219	-0.039849	0.011630
31 C	-0.042874	-0.042157	-0.043918	-0.000717	0.001761	-0.002478
32 H	0.144816	0.149285	0.157127	-0.004469	-0.007842	0.003373
33 H	0.135829	0.143475	0.158096	-0.007646	-0.014621	0.006975
34 O	-0.649627	-0.637871	-0.619648	-0.011756	-0.018223	0.006467
35 H	0.379153	0.395949	0.417465	-0.016796	-0.021516	0.004720
36 Cl	-0.356127	-0.266797	-0.015007	-0.089330	-0.251790	0.162460

It has been reported in the literature that the dual descriptor is more accurate local reactivity descriptor than Fukui function [25]. The paper has shown that although the Fukui function has the capability of revealing nucleophilic and electrophilic regions in a molecule, the dual descriptor is able to unambiguously expose truly nucleophilic and electrophilic regions; moreover, dual descriptor is less affected by the lack of relaxation terms than the Fukui function [25]. For these reasons, we choose to use both quantities (Fukui function and dual descriptor) to determine the local reactivity sites of thiamine chloride. Table 5 also gives the dual descriptor for each atom in the studied molecule.

From Table 5, it is clear that N(18) with the maximum value of f_k^+ and positive value of $\Delta f_k(r)$ is the most probable nucleophilic attack site while C(19) with the maximum value of f_k^- and negative value of $\Delta f k(r)$ is most probable electrophile attack site.

Mechanism of inhibition

The inhibition of the aluminium acid corrosion by thiamine hydrochloride is achieved via thiamine chloride (*TMCl*) which adsorption depends upon its molecular structure, which contains heteroatoms such as nitrogen and oxygen (Table 5) and delocalized π-electrons of heterocyclic ring. In acidic aqueous solution, the inhibitor molecules are transformed in cationic form by releasing chloric ion:

$$[TMCl] \rightarrow [TM]^+ + Cl^- \tag{23}$$
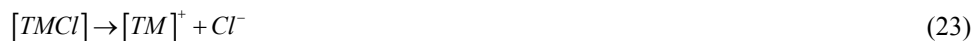
Some of the cationic species could be protonated since they contain heteroatoms:

$$[TM]^+ + H^+ \leftrightarrow [TMH]^{2+} \tag{24}$$

Due to their specific adsorption and their small degree of hydratation, chloride ions (*Cl*)from HCl and that resulting from equation (23) firstly adsorbed on the positively charged metal surface $_{Al^{3+}}$ ions cover the surface of the metal) and create an excess negative charge along the metal surface towards the solution side, what leads to the adsorption of the cationic species and their protonated form. Therefore, a protective layer due to the electrostatic interaction between the charged species from the inhibitor and the chloride ions is formed. The positive sign of fraction of electron transferred shows that electrons can be transferred from the inhibitor species to the aluminium and that positive charges species have a strong tendency to accept electron from p orbital of the aluminium to form a bond, what could explain the existence of the chemisorption. So, a probable schematic mechanism (Figure 10) can be proposed where the black arrows indicate chemisorption, while the broken lines show the electrostatic interaction between the chloride ions and the cationic form of the inhibitor.
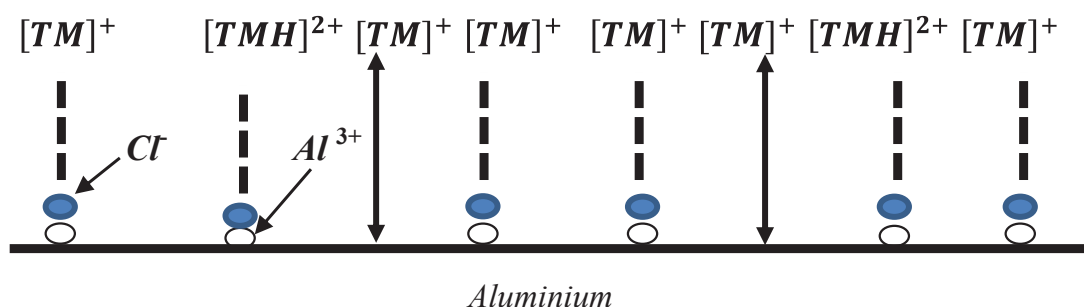
Aluminium

Figure 10: Schematic mechanism of aluminium inhibition in 1.0 M HCl by TMCl

CONCLUSION

Thiamine hydrochloride shows good inhibition properties via thiamine chloride for aluminium corrosion in 1.0 M HCl. The inhibition efficiency increases with increasing concentration in the studied compound but decreases with rise in temperature. Adsorption of thiamine chloride obeys the Langmuir modified adsorption isotherm. The adsorption and activation thermodynamic functions reveal a spontaneous adsorption process of the studied molecule onto aluminium and both physisorption and chemisorption mechanisms. Quantum chemical calculations data from B3LYP/6-31G (d) are in good agreement with experimental results.

REFERENCES

[1] Safak, S., et al., *Corros Sci*, **2012**. 54: p. 251.

[2] Li, X., Deng, S. and Xie, X., *Corros Sci*, **2014**. 81: p. 162.

[3] Hazzazi, O.A. and Abdallah, M., *Int J Electrochem Sci*, **2013**. 8: p. 8138.

[4] El-Haddad, M.N. and Fouda, A.S., *J Mol Liq*, **2015**. 209: p. 480.

[5] Fouda, A.S., et al., *Prot Mat Phys Chem Surf*, **2011**. 47: p. 803.

[6] Hassan, S.M., *Corros Sci*, **1979**. 19: p. 951.

[7] Fouda, S.A., *Corros Sci*, **2008**. 51: p. 485.

[8] Abdallah, M, *Corros Sci*, **2004**. 46: p. 1981.

[9] Gece G, *Corros Sci*, **2008**. 50: p. 2981.

[10] Obot, I.B., Obi-Egbedi, N.O. and Umoren, S.A., *Corros Sci*, **2009**. 51: p. 276.

[11] Abd El-Hakeem, S.M., et al., *Corros Sci*, **2013**. 68: p. 1.

[12] Khaled, K.F. and Al-Qahtani, M.M., *Mater Chem Phys*, **2009**. 113: p. 150.

[13] Xiao-Ci, Y., et al., *Corros Sci*, **2000**. 42: p. 645.

[14] El-Ashry, E.H., et al., *Electrochim Acta*, **2006**. 51: p. 3957.

[15] Frisch, M.J., et al., Gaussian 03, Gaussian Inc. Pittsburgh P.A., **2003**.

[16] Lee, C., Yang, W. and Parr, R.G., *Phys Rev B*, **1988**. 37: p. 785.

[17] Geerlings, P., De Proft, F. and Langenaeker, W., *Chem Rev*, **2003**. 103: p. 1793.

[18] Parr, R. and Yang, W., *J Am Chem Soc*, **1984**. 106: p. 4049.

[19] Parr, R.G., Szentpaly, L. and Liu, S., *J Am Chem Soc*, **1999**. 121: p. 1922.

[20] Kokalj, A., Kovacevic, N., *Chem Phys Lett*, **2011**. 507: p. 181.

[21] Michaelson, H., *J Appl Phys*, **1997**. 48: p. 4729.

[22] Sastri, V.S. and Perumarddi, J.R., *Corrosion*, **1997**, 53: p. 617.

[23] Morell, C., Grand, A. and Torro-Labbé, A., *Chem Phys Lett*, **2006**. 425: p. 342.

[24] Morell, C., Grand, A. and Torro-Labbé, A., *J Phys Chem A*, **2005**. 109: p. 205.

[25] Martinez-Araya, J.I., *Math Chem*, **2015**. 53: p. 451.

[26] Liu, F.G., *Corros Sci*, **2009**. 51: p. 102.

[27] Hammed, R.S.A., et al., *Int J Electrochem Sci*, **2015**. 10: p. 2098.

[28] Villamil, R.F.V., et al., *J Electroanal Chem*, **1999**. 472: p.112.

[29] Adejo, S.O. and Ekwenchi, M.M., *IOSR J Appl Chem*, **2014**. 6: p. 66.

[30] Benabdellah, M., et al., *Mater Lett,* **2007**. 61: p. 1197.

[31] Adejo, S.O., et al., *J Emerg Trends Eng Appl Sci (JETEAS)*, **2014**. 5: p. 201.

[32] Umoren, S.A. and Ebenso, E.E., *Mater Chem Phys*, **2007**. 106: p. 387.

[33] Fouda, A.S., Abd El-Aal, A. and Khandil, A.B., *Desalination*, **2006**. 201: p. 216.

[34] Guan, N.M., Xueming, L. and Fei, L., *Mater Chem Phys*, **2004**. 86: p. 59.

[35] Obi-Egbedi, N.O. and Obot, I.B., *Corros Sci*, **2011**. 53: p. 263.

[36] Gece, G. and Bilgic, S., *Corros Sci*, **2009**. 51: p. 1876.

[37] Obi-Egbedi, N.O. and Obot, I.B., *J Mol Struct*, **2011**. 1002: p. 86.

[38] Ahamad, I., Prasad, R. and Quraishi, M.A., *Corros Sci*, **2010**. 52: p. 1472.

[39] Adejoro, I.A., Ibeji, C.U. and Akintayo, D.C., *Chem Sci J*, **2017**. 8: p. 149.

[40] Ibeji, C.U., Adejoro, I.A. and Adeleke, B.B., *J Phys Chem Biophys*, **2015**. 5: p. 1.

[41] Musa, A.Y., et al., *J Mol Struct*, **2010**. 969: p. 233.

[42] Obot, I.B. and Obi-Egbedi, N.O., *Corros Sci*, **2010**. 52: p. 657.

[43] Khalil, N., *Electrochimica Acta*, **2003**. 48: p. 2635.

[44] Sahin, M., et al., *J. Appl. Electrochem.*, **2008**, 38: p. 809.

[45] Kokalj, A., *Electrochimica Acta*, **2010**. 56: p. 745.

[46] Udhayakala, P., Rajendiran, T.V. and Gunasekaran, S., *J Chem Biol Phys Sci*, **2012**, 2: p. 172.

[47] Parr, R.G., Szentpaly, L.V. and Liu, S., *J Am Chem Soc*, **1999**. 121: p. 1922.

[48] Ozcan, M. and Dehri, I., *Prog Org Coat*, **2004**. 51: p. 181.